Bone 164 (2022) 116526

Contents lists available at ScienceDirect

Bone

journal homepage: www.elsevier.com/locate/bone

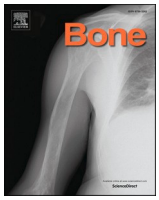

Full length article

Methylglyoxal – an advanced glycation end products (AGEs) precursor – Inhibits differentiation of human MSC-derived osteoblasts in vitro independently of receptor for AGEs (RAGE)

Komal Waqas, Max Muller, Marijke Koedam, Youssra el Kadi, M. Carola Zillikens, B.C.J. van der Eerden *

Department of Internal Medicine, Erasmus MC, Erasmus University Medical Center, Rotterdam, the Netherlands

ARTICLE INFO

Keywords:
Advanced glycation end products
Methylglyoxal
Osteoblasts
Mesenchymal stem cells
Receptor for AGEs

ABSTRACT

A major precursor of advanced glycation end-products (AGEs) - methylglyoxal (MG) - is a reactive carbonyl metabolite that originates from glycolytic pathways. MG formation and accumulation has been implicated in the pathogenesis of diabetes and age-related chronic musculoskeletal disorders. Human bone marrow-derived stromal cells (BMSCs) are multipotent cells that have the potential to differentiate into cells of mesenchymal origin including osteoblasts, but the role of MG on their differentiation is unclear. We therefore evaluated the effect of MG on proliferation and differentiation of BMSC-derived osteoblasts.

Cells were treated with different concentrations of MG (600, 800 and 1000 μM). Cell viability was assessed using a Cell Counting Kit-8 assay. Alkaline phosphatase (ALP) activity and calcium deposition assays were performed to evaluate osteoblast differentiation and mineralization. Gene expression was measured using qRT-PCR, whereas AGE specific receptor (RAGE) and collagen 1 were examined by immunocytochemistry and Western blotting. RAGE knockdown was performed by transducing RAGE specific short hairpin RNAs (shRNAs) using lentivirus.

During osteogenic differentiation, MG treatment resulted in reduction of cell viability (27.7 %), ALP activity (45.5 %) and mineralization (82.3 %) compared to untreated cells. MG significantly decreased expression of genes involved in osteogenic differentiation - *RUNX2* (2.8 fold), *ALPL* (3.2 fold), MG detoxification through glyoxalase - *GLO1* (3 fold) and collagen metabolism - *COL1A1* (4.9 fold), *COL1A2* (6.8 fold), *LOX* (5.4 fold) and *PLOD1* (1.7 fold). MG significantly reduced expression of collagen 1 (53.3 %) and RAGE (43.1 %) at protein levels. Co-treatment with a MG scavenger - aminoguanidine – prevented all negative effects of MG. RAGE-specific knockdown during MG treatment did not reverse the effects on cell viability, osteogenic differentiation or collagen metabolism.

In conclusion, MG treatment can negatively influence the collagen metabolism and differentiation of BMSCs-derived osteoblasts through a RAGE independent mechanism.

1. Introduction

Methylglyoxal (MG) is a highly reactive dicarbonyl compound formed primarily as a byproduct of glycolysis [1] but also during lipid peroxidation and protein degradation. It is a potent glycating agent and a predominant precursor of advanced glycation end products (AGEs) [2]. MG is formed not only during states of chronic hyperglycemia such as in diabetes but also during states of hypoxia and inflammation [3,4]. In addition to the endogenous MG production, diet and cigarette smoking are the exogenous contributors to the body's MG pool [5–7]. It is of note that although the concentration of MG is much lower than glucose in tissues, MG is about 20,000 times more reactive than glucose [8]. The major physiological detoxification mechanism against MG is the glutathione (GSH)-dependent glyoxalase (GLO) system consisting of GLO1, GLO2 and reduced GSH [9]. MG accumulation, either due to enhanced production or due to reduced detoxification, is referred to as 'dicarbonyl stress' [10] and increased accumulation of MG-derived AGEs contribute to the so called 'glycative stress' [11]. Altogether,

* Corresponding author at: Department of Internal Medicine, Erasmus, University Medical Center, 's-Gravendijkwal 230, 3015CE Rotterdam, the Netherlands.
E-mail address: b.vandereerden@erasmusmc.nl (B.C.J. van der Eerden).

https://doi.org/10.1016/j.bone.2022.116526
Received 17 May 2022; Received in revised form 27 July 2022; Accepted 16 August 2022
Available online 19 August 2022

both dicarbonyl and glycative stress have been shown to play a role in promoting age-related chronic inflammatory conditions such as atherosclerosis, osteoporosis, cancer and neurodegenerative diseases [12–15].

MG and MG-derived AGEs have been shown to increase the risk of fracture by several mechanisms including net bone loss by affecting bone remodeling [16], reducing bone matrix quality [17] and possibly delaying bone healing in individuals with diabetes [18]. The molecule 5-hydro-5-methylimidazolone (MGH1) is a key MG-derived AGE and was recently shown to be the most abundant AGE (up to ~200 times higher) in bone compared to other non-MG-derived AGEs in elderly individuals without diabetes [19]. Glycative stress due to MG-derived AGEs has been induced through its binding to the transmembrane receptor for AGEs (RAGE) and downstream activation of Nicotinamide Adenine Dinucleotide Phosphate Hydrogen (NADPH) oxidase and upregulation of nuclear factor κ-β-producing pro-inflammatory cytokines [20]. Also, MG-derived AGEs increase non-enzymatic cross-linking of extracellular matrix (ECM) proteins and alter their structure and function [21] Dicarbonyl stress due to MG has been shown not only to enhance AGEs accumulation but also evoke direct carbonylative damage to intracellular proteins and DNA [10]. As an example, MG-associated carbonylation can be both a cause or consequence of oxidative stress. For example, MG reacting to mitochondrial proteins generates reactive oxygen species (ROS), while depletion of GSH and NADPH during oxidative stress decreases the activity of GLO1 and further enhances MG accumulation. Overall, it seems that MG-associated dicarbonyl and glycative stress may affect bone remodeling both in a RAGE-dependent and –independent manner.

Human bone marrow-derived stromal cells (BMSCs) are a population of self-renewing multipotent cells with capacity to differentiate into several mesenchymal tissues including bone, cartilage, muscle and fat. They are characterized by their ability to remodel and regenerate. In a previous study, treatment of BMSCs with glyceraldehyde-derived AGEs prevented their differentiation into osteoblasts [22]. Until now, there have been no studies on the potential detrimental effects of MG or MG-derived AGEs on proliferation and differentiation of BMSCs-derived osteoblasts. Recently, we observed in our population-based cohort that higher skin AGEs accumulation was associated with higher risk of fracture independent of bone mineral density, which points towards a reduction in bone quality largely influenced through organic matrix predominantly comprising collagen [23]. In this context, the reversibility of the effects produced by MG either through synthetic or natural MG scavengers and GLO1 inducers [24] or through RAGE blockade [25] have been proposed as important future research approaches. However, it is not yet clear to what extent the effects of MG are derived through RAGE.

Therefore, we aimed to investigate whether MG-induced dicarbonyl or glycative stress alters collagen metabolism in BMSCs-derived osteoblasts. We further investigated whether this effect is mediated through RAGE by employing a RAGE-specific knockdown under conditions of high MG concentrations that stimulate dicarbonyl stress.

2. Materials and methods

2.1. Chemicals

Methylglyoxal was purchased as methylglyoxal solution (~40 % in H_2O) from Sigma-Aldrich (cat. M0252). Aminoguanidine was purchased as Aminoguadine hydrochloride from Sigma-Aldrich (cat. MKCL5504). Cell cultures were photographed using Rebel microscope from Echo.

2.2. Cell cultures

Human BMSCs were derived from the bone-marrow of a young male human donor. BMSCs were differentiated into mineralizing osteoblasts as described previously [26]. Briefly, BMSCs were seeded (5000 cells/cm^2) and maintained for first two days in alpha minimum essential medium (α-MEM, Gibco, Paisley, United Kingdom) supplemented with 10 % heat-inactivated fetal calf serum. Next, they were differentiated towards mineralizing osteoblasts α-MEM supplemented with 10 mM β-glycerophosphate (β-GP) and 100 nM dexamethasone for a period of 2–3 weeks. Cells at passage 8 were used in all experiments and the media was refreshed two times a week. Cells were treated with different concentrations of MG varying from 400 to 1000 μM after 3 days of osteogenic induction in comparison to controls (not treated with MG). At the start of our experiments, we compared a dose of 100 μM vs. 400 μM aminoguanidine (AG), which showed that 400 μM AG counteracts MG better than 100 μM AG in reversing the effects on cell viability. These concentrations of AG were based on other studies using different cell models with doses between 100 and 400 μM AG as a MG scavenger [27–29]. Therefore, cells were also treated with 400 μM of AG after 3 days of osteogenic induction simultaneously with MG for all the experiments. All experiments were performed at least two times in quadruplicate per condition and per time point.

2.3. Cell viability assay

Cells were cultured in a 96-well plate at a density of 5000 cells/cm^2 in α-MEM medium containing β-GP and dexamethasone. A cell counting kit assay was performed when cells were mixed with 10 μL of tetrazolium salt WST-8 (2-(2-methoxy-4-nitrophenyl)-3-(4-nitrophenyl)-5-(2,4-disulfophenyl)-2H-tetrazolium, monosodium salt) solution per well and incubated for 2 h at 37 °C. WST-8 is bio-reduced by cellular dehydrogenases to formazan which is released by the cells. The amount of formazan produced is directly proportional to the number of living cells, which was measured at an absorbance of 450 nm by a Perkin Elmer Victor X2 multilabel Microplate Reader (Molecular Devices, Sunnyvale, CA, USA).

2.4. Alkaline phosphatase (ALP) activity

ALP activity was measured at day 7 of osteogenic induction i.e., 96 h after starting treatment with MG. ALP activity was measured by an enzymatic reaction requiring ALP for the conversion of substrate (paranitrophenylphosphate, pNPP) to the product (paranitrophenol, PNP), as described previously [26]. Briefly, cell extracts were harvested using PBS containing 0.1 % triton X-100. The conversion step from pNPP to PNP was performed for 10 min at 37 °C. ALP activity was quantified by measuring the absorbance at 405 nm using the Perkin Elmer Victor X2 multilabel Microplate Reader and the results were adjusted for protein content of the cell lysates also measured at day 7.

2.5. Calcium assessment in cell culture

For calcium measurements, cell lysates and the residual ECM material in the plates were incubated overnight with 0.24 M HCl at 4 °C. Calcium content was determined colorimetrically using a calcium assay reagent prepared by combining 1 M ethanolamine buffer (pH 10.6) with 0.35 mM O-cresolphthalein complex one in a ratio of 1:1 and 9,8 mM 8-hydroxyquinoline (SIGMA 252565-50G, Lot#128M4049V) en 0,6 M HCL. All measurements were performed using a Perkin Elmer Victor X2 multilabel Microplate Reader. Von Kossa staining was performed as described previously [25]. Briefly, cells were fixed with 70 % ethanol and stained for 15 min with von Kossa solution at RT (pH 4.2, Sigma-Aldrich, St. Louis, Missouri, United States).

2.6. Methylglyoxal-modified protein adducts quantified by ELISA

MG-H1 protein adducts were measured by using a competitive enzyme-linked immunosorbent assay (ELISA) kit (OxiSelect™ Methylglyoxal competitive ELISA STA-811 Cellbiolabs) according to the manufacturer's instructions.

2.7. Gene expression quantified by real-time polymerase chain reaction (PCR)

Total mRNA isolation and cDNA synthesis was performed as described earlier [26]. Briefly, RNA extraction was performed using TRIzol reagent at different time points treated with different MG concentrations varying from 0 to 800 μM. After RNA purification, cDNA was synthesized using Reverse transcriptase (RT) and adding poly-T oligonucleotide primer to the mature mRNA. Real time quantitative PCR was performed using Quantstudio 7 flex Taqman and the results were analyzed using QuantStudio™, Real time PCR software version 1.3 (Applied Biosystems by Thermo Fischer Scientific). We expressed mRNA levels of a respective gene relative to the expression of a housekeeping gene GAPDH on the basis of the following formula: $2^{-\Delta(\text{Ct of gene of interest} - \text{Ct of housekeeping gene})}$. Supplementary Table 1 shows the forward and reverse primer sequences of the analyzed genes.

2.8. Immunocytochemistry

Immunocytochemistry was performed as previously described [30]. Briefly, BMSCs were fixed with 4 % PFA for 5 min at RT and washed with PBS. Immunostaining was performed after permeabilization with 0.1 % Triton X-100 (Sigma-Aldrich, St. Louis, Missouri, United States) in PBS and blocking for 30 min in 1 % bovine serum albumin at RT simultaneously. Cells were incubated with anti-RAGE Antibody (9A11) (1:100; Santa Cruz Biotechnology) or anti-COL1A1 antibody (1:100; Southern Biotech, #1440-1, clone 2A3, mouse-anti-human) overnight at 4 °C. The next day, cells were incubated with Alexa Flour 488 donkey anti-mouse (1:200; Abcam, Cambridge, United Kingdom) secondary antibody for 1 h at RT, followed by the addition of rhodamine-conjugated phalloidin (1:100, Thermo Fisher Scientific, Massachusetts, United States) for 1 h at RT. After 10 min incubation with 4′,6-diamidino-2-phenylindole (DAPI), images were taken with an AxioObserver microscope (Zeiss).

2.9. Total protein isolation and Western blotting

Western blot analysis was performed as described [28]. Total protein was collected in RIPA lysis buffer (1:100, Thermo Fisher Scientific, Massachusetts, United States). Equal amounts of protein per sample were loaded and separated by SDS-PAGE (Bio-Rad Laboratories B.V., Veenendaal, The Netherlands) and transferred onto a polyvinylidene difluoride membrane (Amersham™ Hybond® Western blotting membranes, Sigma-Aldrich, Zwijndrecht, the Netherlands). Each membrane was blocked with 5 % non-fat milk in Tris-buffered saline containing 0.1 % Tween-20 (TBS-T) at RT for 1 h before blotting with primary antibodies directed against RAGE (1:1000; Santa Cruz Biotechnology), β-Actin (1:1000; Cell signaling, Leiden, The Netherland.s) and COL1A1 (1:1000; Santa Cruz Biotechnology) at 4 °C overnight. After three washes in TBS-T, the membrane was incubated with anti-mouse antibody (1:2000; Cell signaling, Leiden, The Netherlands) conjugated with horse radish peroxidase for 1 h at RT. The proteins of interest were detected with a Gel Doc XR System (Bio-Rad Laboratories B.V., Veenendaal, The Netherlands) using the Clarity™ Western ECL Substrate (Bio-Rad Laboratories B.V., Veenendaal, The Netherlands) and were semi-quantified using Image Lab software (Bio-Rad Laboratories B.V., Veenendaal, The Netherlands). Blots were re-used to measure the aforementioned three proteins namely, β-Actin, COL1A1 and RAGE in the same samples. Following RAGE antibody probing on the membrane and detection, the blot was stripped using a strip buffer to allow for the primary antibody for COL1A1 to be applied, and finalized by using the β-Actin antibody.

2.10. Short hairpin-mediated knockdown by lentiviral transduction

The constructs of short hairpin RNA (shRNA) targeting RAGE and the non-targeting shRNA with a scrambled sequence serving as negative control were purchased from TRC-1.0 library (Sigma-Aldrich, Zwijndrecht, the Netherlands; Table S1). Lentiviral transduction was performed using the ViraPower packaging vector plasmids (Thermo Fisher scientific). Lentivirus was produced by transient transfection into 293FT cells using a standard calcium phosphate precipitation method [25]. After 24 h, supernatants containing lentivirus were harvested, and used immediately for hMSC transduction (24 h after attachment). One day later, medium was replaced with osteogenic induction medium, and cells were cultured until further analysis. All aforementioned assays were performed in the scrambled and RAGE-shRNA transduced cells.

3. Results

3.1. Methylglyoxal impairs cell growth in BMSCs derived pre-osteoblasts

MG has been shown to induce apoptosis and affect cell proliferation in various human osteoblastic and non-osteoblastic cell lines [31,32]. Here, we wanted to investigate whether a similar response could be seen in our MG-treated BMSCs-derived osteoblasts. Compared with controls, an MG concentration of 800 μM caused a significant 27.7 % decrease in cell viability, whereas 1000 μM MG reduced cell viability to 84.3 % as shown in Fig. 1A. Lower concentrations such as 400 and 600 μM MG did not cause a significant decline in cell viability in our pre-osteoblasts. Lastly, co-treatment of cells simultaneously with 800 μM MG and 400 μM AG (as positive control) reversed the effects of MG and showed no difference in cell viability versus controls (Figs. 1A and B). Our results suggest that 800 μM MG is an optimal dose that induces effects on cell viability.

3.2. Methylglyoxal induces glycative stress

Glycative stress is a metabolic condition characterized by abnormally high accumulation of AGEs. We assessed accumulation of intracellular AGEs as MG-derived protein adducts and the glyoxalase system assessing gene expression of *GLO1*, *GLO2* and *GSR*. MG led to 2.7 fold higher intracellular accumulation of MG-derived protein adducts compared with controls, as measured by immunoassay (Fig. 2A). This increased accumulation of MG-derived AGEs has been shown to be partially increased through inhibition of the glyoxalase system, which is a major MG detoxifying mechanism of the cells [9]. Exposure to MG for first 24 h resulted in a 3-fold decrease in GLO1 (Fig. 2B) and GSR expression (Fig. 2C). At 96 h, gene expression of both *GLO1* and *GSR* did not differ between MG and controls whereas GLO2 decreased only at that time point (Fig. 2D). Altogether, these results point towards the fact that MG induces glycative stress due to AGEs formation in BMSC-derived pre-osteoblasts and that it may partially be mediated through initial inhibition of *GLO1* and *GSR*.

3.3. Methylglyoxal inhibits osteoblast differentiation

Inhibition of osteoblastic differentiation could influence BMSCs-derived bone remodeling and bone regeneration during (micro-)fracture healing in a negative manner [33,34]. So, we assessed osteoblastic differentiation and mineralization and measured the activity of the osteoblast differentiation marker ALP, deposition of calcium and expression of osteoblast differentiation genes. MG led to a 55.5 % (2.2 fold) reduction in ALP activity at 96 h (Fig. 3A) and to a 47.9 % (1.9 fold) reduction in the amount of incorporated calcium at day 20 (Fig. 3B), which was confirmed by von Kossa staining (Fig. 3C). Of note, we did not find a significant downregulation of *RUNX2* or *ALPL* at 24 h (Figs. 3D and E). However, both *ALPL* and *RUNX2* expression were downregulated by MG later during differentiation (96 h or day 11).

3.4. Methylglyoxal inhibits collagen formation and breakdown

AGEs accumulation has been linked to the formation of non-

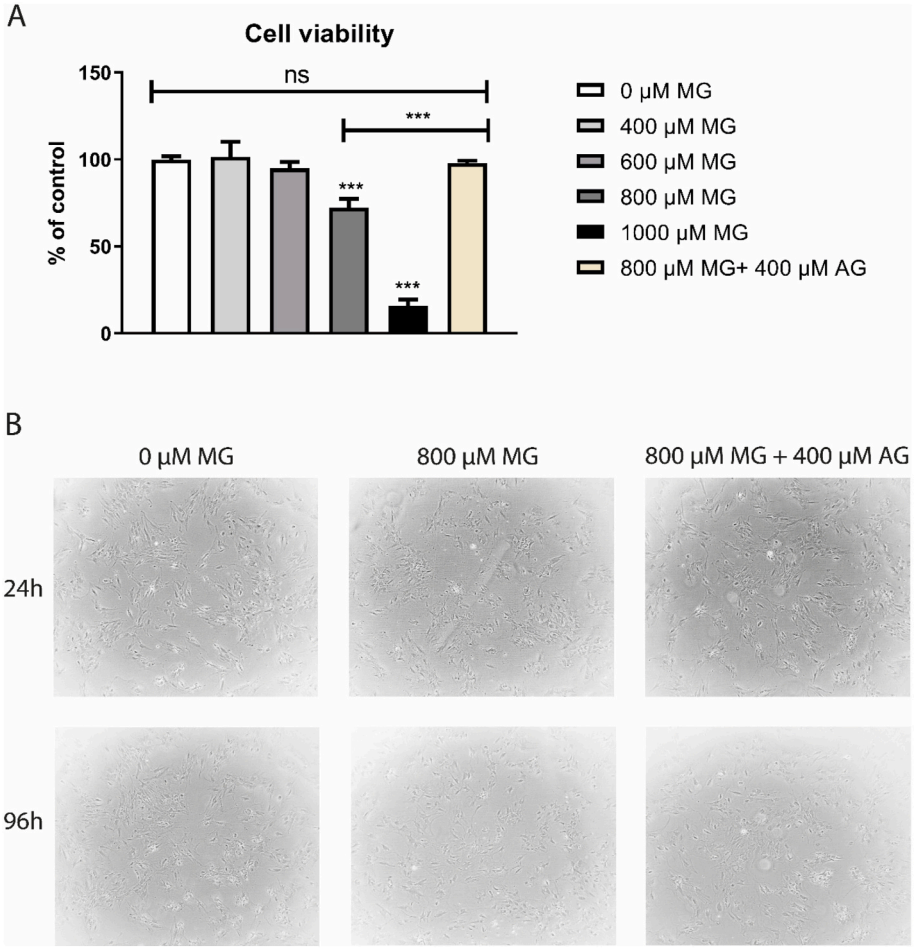

Fig. 1. Methylglyoxal (MG) impairs cell viability in BMSCs-derived pre-osteoblasts which is reversible upon co-treatment with aminoguanidine. (A) Cell viability as measured by CCK-8 assay at 96 h when treated with 400 μM, 600 μM, 800 μM, 1000 μM and 800 μM MG + 400 μM aminoguanidine (AG) compared to controls. (B) Representative morphological images of BMSCs-derived osteoblasts at 24 h and 96 h of culture in MG treated cells vs. controls. All experiments are performed twice with $N = 4$ for every condition. Error bars represent the standard error of the mean. ns, not significant, $^{***}p < 0.0001$, ns; not significant.

enzymatic crosslinks in the extracellular matrix of bone, which increases bone stiffness and decreases bone quality leading to an increased risk of fracture independent of bone quantity [23,35,36]. To clarify whether MG can also affect collagen metabolism in BMSCs-derived osteoblasts, we assessed collagen levels by immunostaining and Western blotting and additionally the mRNA expression of genes involved in collagen formation (*COL1A1* and *COL1A2* - Fig. 4A and B), crosslinking (lysyl oxidase, *LOX* and lysyl hydroxylase, *PLOD1* – Fig. 4C and D) and breakdown (metalloproteinase 2, *MMP2* and tissue inhibitor of metalloproteinases 1, *TIMP1* – Fig. 4E and F). Following treatment with MG, the expression of collagen metabolism related genes was downregulated at all time points when compared with controls - *COL1A1* (5.2 fold), *COL1A2* (14.1 fold), *LOX* (5.4 fold), *PLOD1* (2.1 fold) and *MMP2* (3.9 fold) except *TIMP1*, which showed no significant change at all included time points (24 h, 96 h or day 11) (Figs. 4A-F). Immunocytochemical staining with an anti-collagen antibody did not appear to show less collagen 1 staining following MG treatment at day 11 (Fig. 4G) but quantification is a refined approach. Hence, we proceeded with Western blot to allow for quantification and it showed a significant decrease in collagen protein (−53.3 %) relative to actin (Fig. 4H). Our results suggest a decrease in collagen expression at protein levels in MG-treated cells with indications from mRNA expression data that this decrease in collagen was primarily due to downregulation of genes related to fibril formation and crosslinking rather than increased breakdown.

3.5. Methylglyoxal induces inflammatory stress but downregulates RAGE expression

MG, primarily through the interaction of MG-derived AGEs as a ligand for RAGE, has been shown to induce pro-inflammatory stress [37,38]. Therefore, we investigated whether MG could also induce inflammation in BMSCs-derived osteoblasts through the measurement of mRNA expression of prominent inflammatory cytokines, namely *IL-6* and *IL-1β*. Also, we evaluated whether this response was paralleled by changes in RAGE expression. As shown in Fig. 5, MG led to a significant robust upregulation of *IL6* (51 fold) but no change in *IL1β* (1.4 fold) expression (Fig. 5B–C) while it considerably reduced RAGE expression at mRNA (4.1 fold) (Fig. 5A). Immunocytochemistry results appeared to show reduced RAGE expression following MG treatment at day 11, which normalized with the additional AG treatment (Fig. 5D). These data were further substantiated at day 11 by Western blotting and a relative 43 % decrease in the RAGE intensity compared to controls (Fig. 5E). Altogether, our results point towards a pro-inflammatory role of MG, while RAGE levels were markedly decreased.

3.6. RAGE-specific knockdown did not reverse MG-induced pre-osteoblast reduction in cell viability and differentiation

In order to differentiate whether the effects of MG are mediated through RAGE or RAGE-independent mechanisms, we performed lentiviral mediated RAGE knockdown by using 5 distinctive shRNAs and a scrambled sequence (Scr) as control (Supplementary Fig. 1). Based on this, we selected two shRNA sequences that resulted in most effective RAGE-specific knockdown as seen by a significant decline in RAGE expression (up to 80 %). Cell viability did not improve when MG treatment was performed in the RAGE shRNAs conditions compared to controls (Fig. 6A). Instead, MG-treated cells showed significantly less cell viability (40–50 % vs. 85 % in controls) when RAGE was knocked

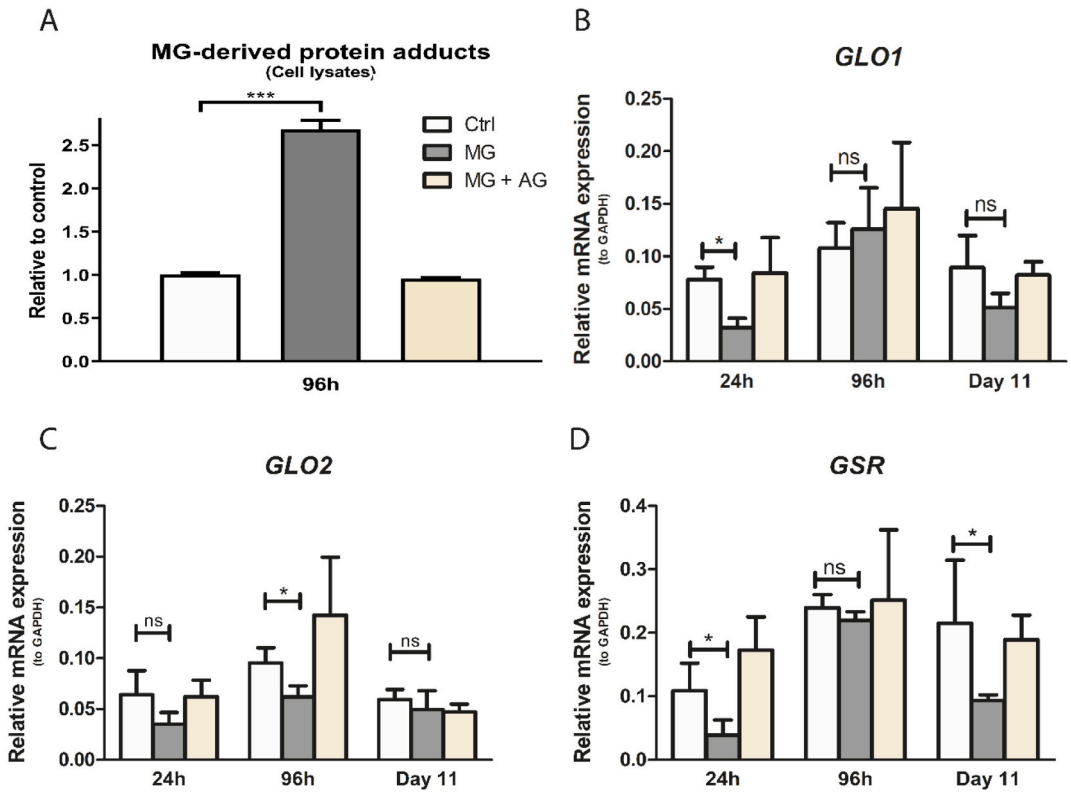

Fig. 2. Methylglyoxal (MG) induces formation of MG-derived protein adducts and inhibits glyoxalase system which is reversible upon co-treatment with aminoguanidine. (A) Glycative stress as measured by ELISA kit for quantification of MG derived protein adducts at 96 h after treating with 800 μM MG and/or 400 μM aminoguanidine compared to controls. mRNA expression using qPCR analysis for (B) GLO1 (C) GLO2 and (D) GSR in controls vs. MG treated cells. Gene expression was corrected in all cases for housekeeping gene GAPDH. All experiments are performed twice with $N = 4$ for every condition. Error bars represent the standard error of the mean. ns, not significant, $*p < 0.05$ and $***p < 0.0001$.

down (Fig. 6A). RAGE knockdown in MG treated cells did not recover ALP activity when compared with MG treated scrambled controls, but this did not reach significance (Fig. 6B). Interestingly, RAGE-specific knockdown resulted in 1.5 to 2.1 fold higher accumulation of intracellular MG-derived AGEs in MG treated cells compared to controls (Fig. 6C). Immunostaining for RAGE confirmed reduced protein expression in RAGE following RAGE shRNAs versus scrambled, which was evident for the controls (Fig. 6D; left panels) and in the co-treatment condition of MG and AG (Fig. 6D, right panels). However, the use of shRNAs against RAGE in combination with MG treatment did show a robust decrease in cell viability but not a distinct reduction in signal of RAGE protein expression when compared to MG treated scrambled controls. However, this absence of reduced RAGE protein expression is most likely due to the relative accumulation of signal due to limited viability of cells in that specific condition (Fig. 6D; middle panels). Immunostaining for collagen did not appear to show any difference in staining intensity following RAGE knockdown versus scrambled controls (Fig. 6E; left bottom versus left upper panels) but the strong reduction in collagen staining in the MG treated samples which was largely reversed by the AG treatment (Fig. 6E, right panels vs middle panels). Altogether, RAGE-specific knockdown resulted in increased accumulation of intracellular MG-derived AGEs in MG-treated cells along with reduced cell viability but comparable ALP activity when compared to scrambled controls. These results point towards a direct action of MG on cellular processes which is not reversed by a RAGE knockdown.

4. Discussion

In the present study, we demonstrate that MG, a major AGEs precursor, inhibited osteoblast differentiation by inducing dicarbonyl/glycative stress and inhibiting collagen metabolism, which did not appear to be mediated through RAGE. Before reaching this conclusion, we showed that MG treatment of BMSCs-derived osteoblasts led to RAGE downregulation while inhibition of RAGE by using a RAGE-specific knockdown did not reverse the effects of MG on osteoblast differentiation. As AG is a well-known MG scavenger known to inhibit AGEs formation [39], we found that AG significantly improved cell viability and differentiation of osteoblasts most likely by reducing intracellular MG-derived AGEs accumulation.

MG exists either as a free dicarbonyl or due to its high reactivity, it binds to arginine or lysine residues on proteins forming AGE adducts in a physiological environment. MG concentration in vivo has been reported to be 0.5–1 μM in healthy individuals and can increase from a few μM up to 300 μM in those with poorly controlled diabetes [40–42]. Similarly, intracellular levels of MG-modified proteins have been reported up to a few hundred μM [43]. Although the concentration of MG in plasma is ~25,000-fold lower than that of glucose, MG is up to 20,000-fold more reactive than glucose with regard to glycation of proteins. MG-H1 levels, a MG-arginine-derived AGE, were found to be higher than CML (a lysine-derived AGE) in femurs of diabetic mice, while similar levels were observed for both AGEs in sera [18]. A very recent report estimated MG-H1 content in human non-diabetic bone samples for the first time and reported it to be the most abundant AGE among other AGEs namely CML, CEL, CMA and up to 2000 times higher in concentration than pentosidine [19]. Therefore, we emphasize that the choice of MG and the concentrations used in our experimental conditions were close to (a) physiological range.

4.1. MG affects osteoblast differentiation and bone health

We found that MG dose-dependently induced reduction in cell viability and inhibited differentiation of human BMSCs-derived

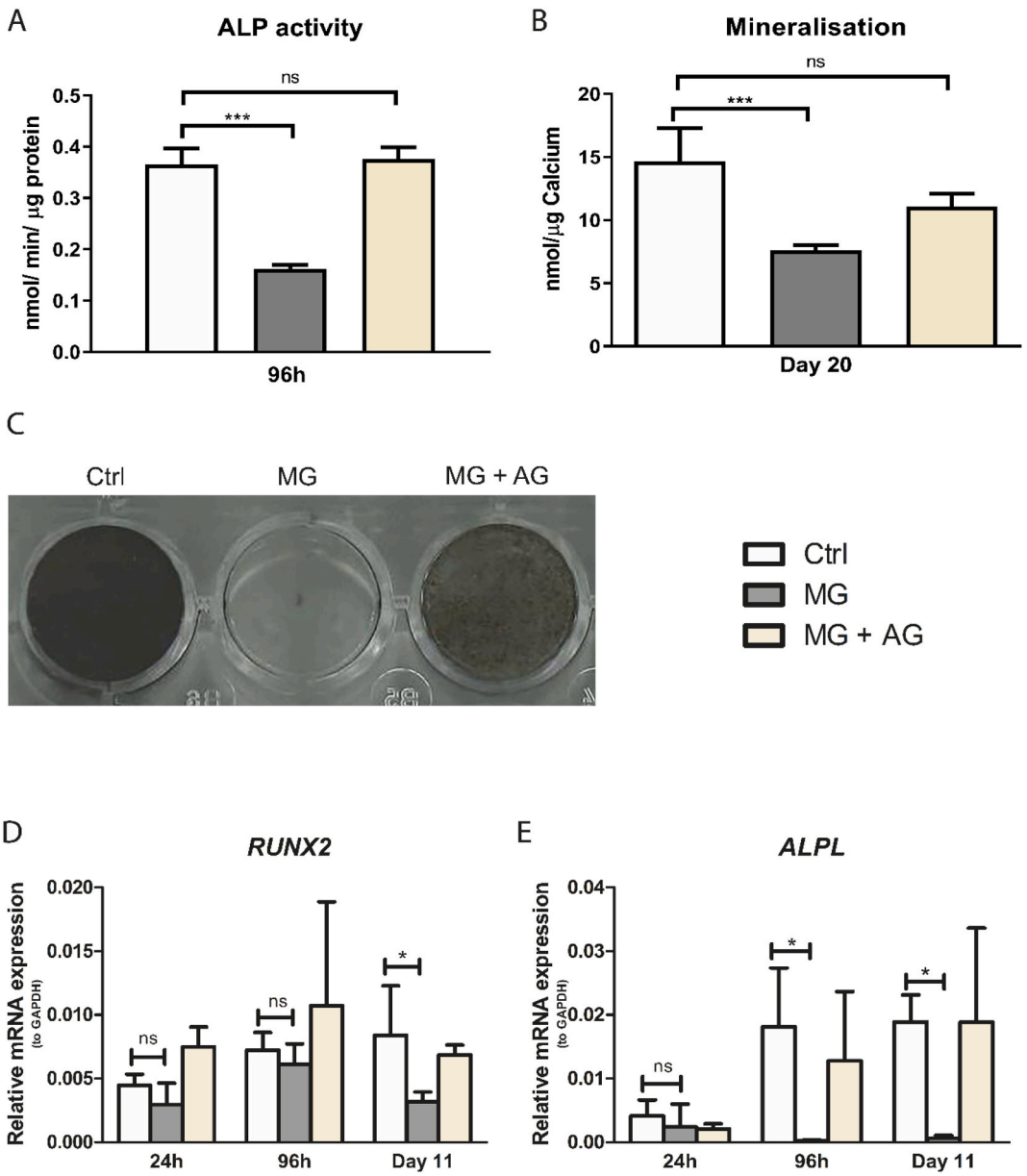

Fig. 3. Methylglyoxal (MG) inhibits both early and late osteoblast differentiation which is reversible upon co-treatment with aminoguanidine. (A) ALP activity at 96 h (B) mineralization through incorporated calcium assay and (C) Von Kossa staining at day 20 after starting treatment with 800 µM MG and/or 400 µM aminoguanidine compared to controls. mRNA expression using qPCR analysis at 24 h, 96 h and day 11 for (D) RUNX2 (E) ALPL in controls vs. MG treated cells. Gene expression was corrected in all cases for housekeeping gene GAPDH. All experiments are performed twice with $N = 4$ for every condition. Error bars represent the standard error of the mean. ns, not significant, $*p < 0.05$ and $***p < 0.0001$.

osteoblasts, which is in line with results obtained in other osteoblastic cell models including humans [31,44]. Undifferentiated BMSCs have been shown to be an important constituent in skeletal homeostasis in adult life [33] and for bone regeneration during fracture repair [34,45]. Both animal and human studies showed that there was a specific decrease in the number of BMSCs with osteogenic capacity during aging but also in mice with T2DM compared with age-matched controls [46–48]. Diabetic mice showed delayed healing following bone injury owed in part to higher accumulation of MG and MG-H1 in their bones compared with non-diabetic controls [18]. Furthermore, *Rage* knockout mice model showed a greater capacity of BMSCs to differentiate into mesenchymal lineages, such as adipocytes and osteocytes [49]. In a different but related context, conditioned medium containing MG-H1 from prostate cancer cells was shown to reprogram human primary OB into a less-differentiated, mesenchymal-like phenotype, which was reversed using aminoguanidine and glo1 silencing [50]. These studies, including ours, provide clues towards MG and AGE-RAGE involvement during MSC differentiation that may act as a mediator in aging, inflammation and diabetic bone phenotypes.

4.2. MG affects collagen metabolism

We demonstrated that following treatment with MG, levels of extracellular matrix (ECM) components including collagen I decreased but also MMP2 expression decreased to a greater extent than tissue inhibitor of matrix metalloproteinase (TIMP1). This may indicate a net decrease in the breakdown of existing collagen. Also, we showed a robust decrease in collagen expression already at 24 h after MG treatment, which was not the case for other osteoblast differentiation genes as *ALPL* and *RUNX2* and their expression and activity decreased only

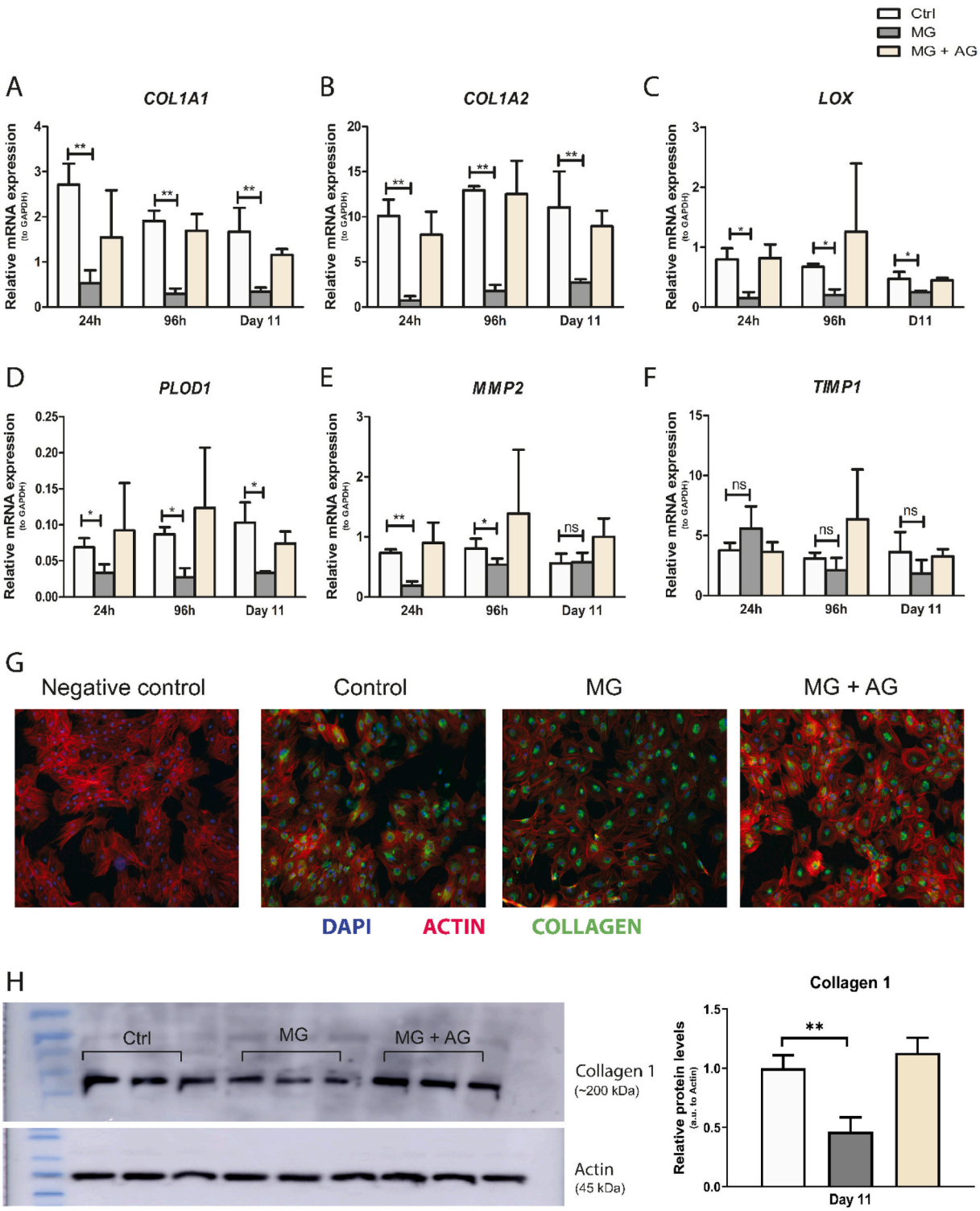

Fig. 4. Methylglyoxal (MG) inhibits collagen formation and breakdown which is reversible upon co-treatment with aminoguanidine. mRNA expression using qPCR analysis at 24 h, 96 h and day 11 for (A) COL1A1 (B) COL1A2 (C) LOX (D) PLOD1 (E) TIMP1 (F) MMP2 in controls vs. MG treated cells. Gene expression was corrected in all cases for housekeeping gene GAPDH. (G) Immunocytochemistry using DAPI/COL1A1/ACTIN(Phalloidin) staining (H) Western blotting using anti-COL1A1 antibody at day 11 in controls vs. MG and/or aminoguanidine treated cells. β-Actin was used to correct the protein expression. All experiments are performed twice with $N = 4$ for every condition. Error bars represent the standard error of the mean. ns, not significant, $^{*}p < 0.05$ and $^{**}p < 0.001$.

after longer treatment with MG. This may point towards a primary effect on altered collagen metabolism causing a delay in differentiation measured with mineralization occurring only later as a consequence, as sometimes observed in some forms of osteogenesis imperfecta [51]. Similar findings were reported explaining bone fragility in individuals with type 2 diabetes whom had normal or high bone mineral density but low bone quality based on abnormal microarchitecture and increased AGEs accumulation on collagens [35]. All in all, our findings suggest not only a decrease in newly formed collagen but also a reduction in breakdown of existing collagen, which may potentially lead to increased

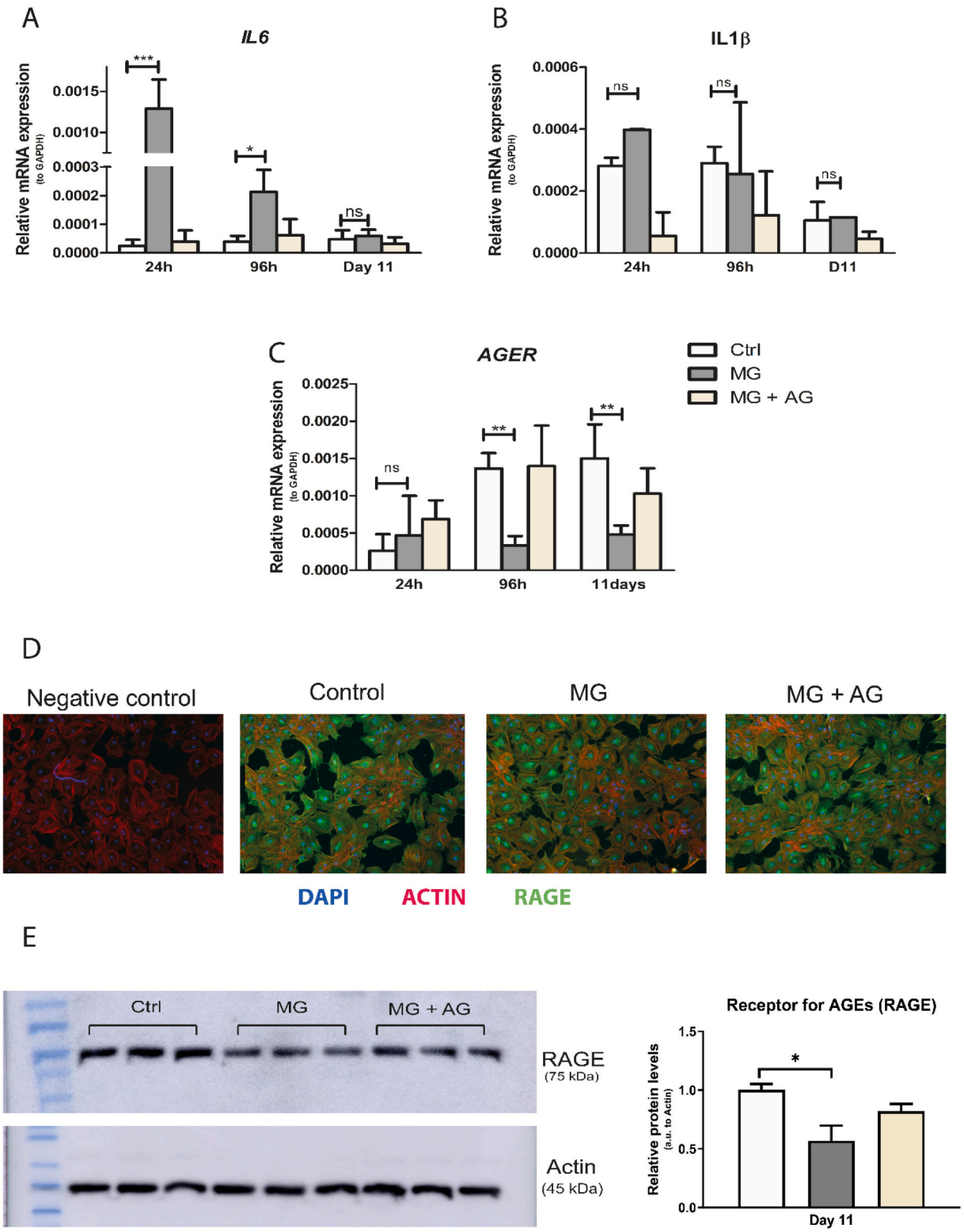

Fig. 5. Methylglyoxal (MG) induces inflammatory stress but downregulates RAGE expression. mRNA expression using qPCR analysis at 24 h, 96 h and day 11 for (A) AGER (B) IL-6 (C) IL-1β (D) Immunocytochemistry using DAPI/RAGE/ACTIN staining (C) Western blotting using anti-RAGE antibody at day 11 in controls vs. MG and/or aminoguanidine treated cells. β-Actin was used to correct the protein expression. All experiments are performed twice with $N = 4$ for every condition. Error bars represent the standard error of the mean. ns, not significant, $^{*}p < 0.05$, $^{**}p < 0.001$ and $^{***}p < 0.0001$.

AGEs crosslinks and risk of fracture.

4.3. MG affects glyoxalase system

The interplay between MG treatment and the glyoxalase system has been studied previously. We also showed that MG treatment of BMSCs

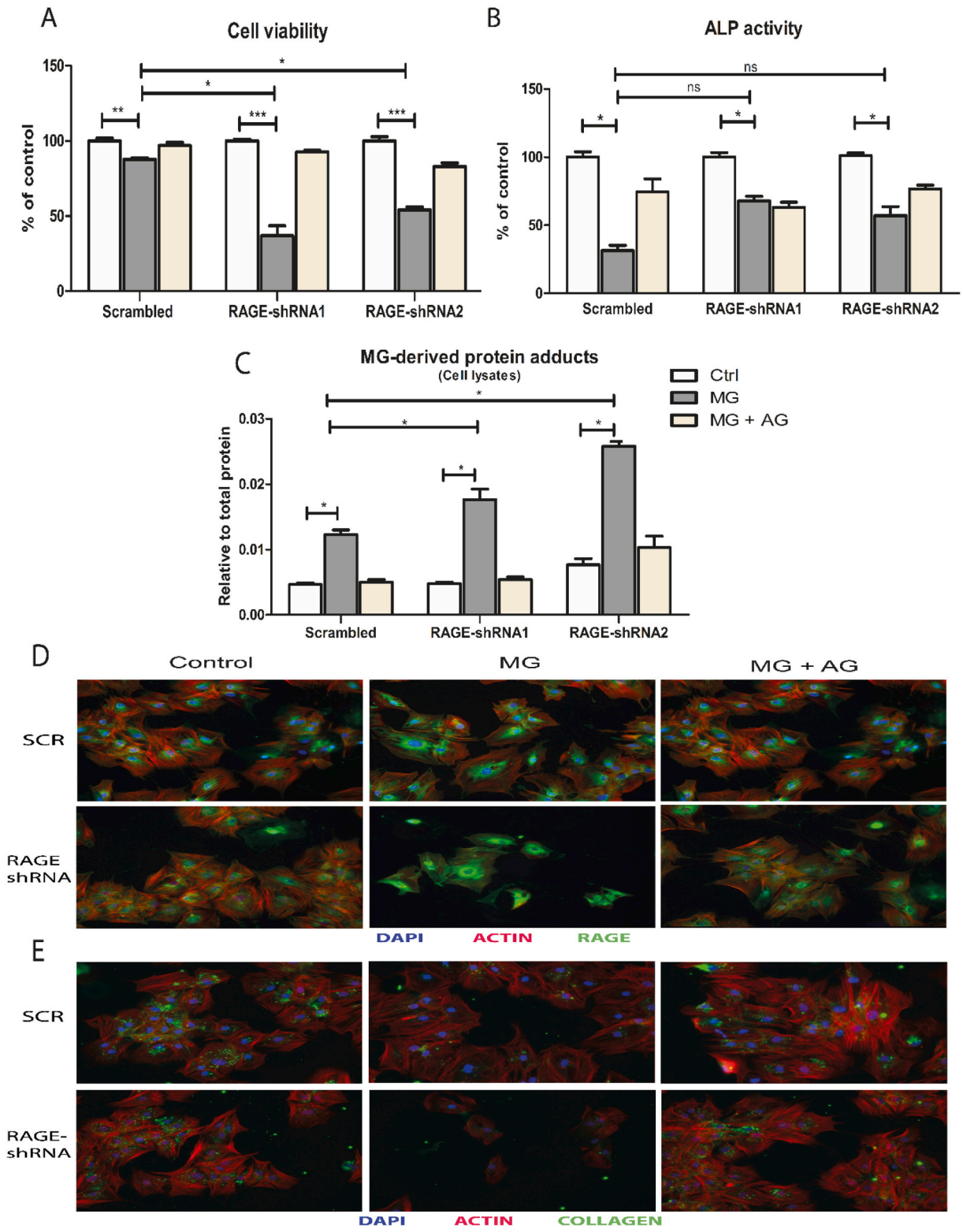

Fig. 6. RAGE knockdown did not reverse the MG induced impaired cell viability and differentiation in osteoblasts. BMSCs-derived osteoblasts were transfected for 72 h with scrambled sequence and RAGE specific shRNA before starting treatment with MG. Effects were measured at (A) cell viability using CCK-8 (B) ALP activity (C) MG-derived protein adducts using ELISA at 96 h in controls vs. MG and/or aminoguanidine treated cells in scrambled and RAGE-specific shRNA conditions. Immunocytochemistry for (D) RAGE and (E) Collagen 1 at day 11 in controls vs. MG and/or aminoguanidine treated cells in scrambled and RAGE-specific shRNA1 conditions. All experiments are performed twice with $N = 4$ for every condition. Error bars represent the standard error of the mean. *$p < 0.05$, **$p < 0.001$ and ***$p < 0.0001$, ns; not significant.

led to an initial downregulation of *GLO1* and *GSR* compared with untreated cells. This was paralleled by an increase in the accumulation of MG-derived AGEs, which further enhances glycative stress in BMSCs. Previously, it was shown that MG-induced oxidative stress led to desensitization of the Nrf2 pathway and downregulation of *GLO1* resulting in reduced detoxification of MG [32]. Besides, Nrf2 silencing has also been shown to reduce *GSR* and in turn, reduce levels of glutathione (GSH) [52], that spontaneously conjugate with MG before it can be detoxified by *GLO1*. Lastly, although Nrf2 is known as a regulator of modest oxidative stress [53], overproduction of ROS can lead to Nrf2 suppression, which eventually downregulates *GLO1* and *GSR* [54,55] as observed here. Nevertheless, in our cells longer treatment with MG did not alter the expression of *glyoxalase*-related genes, which may be due to the fact that cells recovered from the initial stress at that stage and might be able to detoxify MG.

4.4. MG induces inflammatory stress

MG-H1, an MG adduct that serves as a high affinity ligand for RAGE [56], was shown to elicit a pro-inflammatory effect downstream of RAGE. Consistent with other studies, we have demonstrated that MG treatment led to upregulation of the pro-inflammatory cytokines IL-6 and IL-1β [32] and an increased accumulation of intracellular MG-derived protein adducts and downregulation of *GLO1* [57,58]. However, these effects were paralleled by a decrease in RAGE mRNA and protein in our study while a few other studies have shown an increase in RAGE with AGEs treatment [22,59,60]. This suggests that the observed enhanced inflammation or glycative stress and suppression of the glyoxalase system produced by MG might occur in a RAGE-independent manner [61] requiring further investigation.

4.5. RAGE knockdown did not reverse the effects produced by MG on cell viability and osteoblast differentiation

This was why we performed silencing of RAGE with RAGE shRNAs. We demonstrated that the effects of MG on osteoblast differentiation could not be reversed, not even to some extent. In contrast, there was a further 1.6 fold decrease in cell viability and approximately 1.5 fold increase in intracellular MG-derived AGEs following MG treatment in RAGE-silenced cultures, which may point towards a protective role of RAGE. Until now, most of the studies including ours have converged their focus on the pathological role of RAGE. However, recent evidence suggests a physiological role of RAGE in inflammation resolution [62–64]. An intricate balance of cell survival is mediated through RAGE depending on the extent of its stimulation through AGEs – low dose chronic exposure promotes autophagy and inhibition of apoptosis [65–67] and acute high dose exposure stimulates apoptosis and excessive autophagy. Based on this, a possible explanation of RAGE-independent effects of MG in our study could be that MG produced its effects largely by affecting the structure and function of intracellular proteins before extracellular AGEs could be formed, as shown by Suzuki et al., using glyoxal – another dicarbonyl AGEs precursor [68]. Only a small proportion of MG may have been converted extracellularly to MG-derived AGEs, which bind to RAGE and may serve to counteract the excessive inflammation. Taken together, our results suggest that MG acts predominantly through its intracellular effects rather than extracellular MG-AGE-RAGE interactions.

A few other aspects need consideration with respect to MG and RAGE independent signaling in our experimental setup. Whether the binding of MG adducts to RAGE produces downstream signaling and inflammatory response, has been challenged in some recent studies [69,70]. An alternate pathway could be that MG-induced cell stress leads to release of other RAGE ligands such as high mobility group box 1 protein (HMGB1). Low levels of this HMGB1 and RAGE activation has been associated with osteoblast differentiation and fracture healing [71,72]. Overall, these explanations deserve further investigation.

5. Conclusions

The present results provide evidence that BMSCs-derived osteoblasts were inhibited in their proliferation and differentiation by MG treatment with a prominent effect on collagen metabolism. Co-treatment with aminoguanidine prevented these effects. However, RAGE knockdown was unable to protect the osteoblasts from the glycative and inflammatory stress induced by MG.

In practice, natural MG scavengers and RAGE antagonists are being tested commercially to inhibit the effects of AGEs and their precursors on the progression of diabetes and age-related chronic musculoskeletal disorders. Our results suggest to exercise caution when using RAGE antagonists to combat the effects of MG due to possible RAGE-independent effects.

CRediT authorship contribution statement

KW, MCZ and BE designed the study. BE, MK, YK and MM provided essential materials. KW, MM and YK conducted the experiments, assessed and (statistically) analyzed the data. KW, MM and BE interpreted the results. KW created the figures and tables. KW drafted the manuscript. MCZ and BE supervised the manuscript preparation. All authors provided intellectual content to the manuscript. All authors have read and revised the manuscript and approved the final submitted version.

Funding

The Jaap Schouten Foundation, Rotterdam, The Netherlands, kindly provided funding for investigating the role of Advanced Glycation End Products in musculoskeletal health. The funding source had no role in the study design, conducting the experiments, data analysis, and interpretation, writing of the report, or decision to submit the article for publication.

Declaration of competing interest

KW, MM, MK, YK, MCZ and BE declare no conflicts of interest related to this study.

Data availability

Data will be made available on request.

Appendix A. Supplementary data

Supplementary data to this article can be found online at https://doi.org/10.1016/j.bone.2022.116526.

References

[1] I. Allaman, M. Bélanger, P.J. Magistretti, Methylglyoxal, the dark side of glycolysis, Front. Neurosci. 9 (2015) 23.
[2] R. Singh, A. Barden, T. Mori, L. Beilin, Advanced glycation end-products: a review, Diabetologia 44 (2) (2001) 129–146.
[3] P. Matafome, T. Rodrigues, C. Sena, R. Seiça, Methylglyoxal in metabolic disorders: facts, myths, and promises, Med. Res. Rev. 37 (2) (2017) 368–403.
[4] P. Matafome, C. Sena, R. Seiça, Methylglyoxal, obesity, and diabetes, Endocrine 43 (3) (2013) 472–484.
[5] C. Cerami, H. Founds, I. Nicholl, T. Mitsuhashi, D. Giordano, S. Vanpatten, et al., Tobacco smoke is a source of toxic reactive glycation products, Proc. Natl. Acad. Sci. U. S. A. 94 (25) (1997) 13915–13920.
[6] J. Uribarri, M.D. del Castillo, M.P. de la Maza, R. Filip, A. Gugliucci, C. Luevano-Contreras, et al., Dietary advanced glycation end products and their role in health and disease, Adv. Nutr. 6 (4) (2015) 461–473.
[7] J. Uribarri, S. Woodruff, S. Goodman, W. Cai, X. Chen, R. Pyzik, et al., Advanced glycation end products in foods and a practical guide to their reduction in the diet, J. Am. Diet. Assoc. 110 (6) (2010) 911–916, e12.
[8] P.J. Thornalley, Dicarbonyl intermediates in the maillard reaction, Ann. N. Y. Acad. Sci. 1043 (2005) 111–117.

[9] D.E.M. Maessen, C.D.A. Stehouwer, C.G. Schalkwijk, The role of methylglyoxal and the glyoxalase system in diabetes and other age-related diseases, Clin. Sci. 128 (12) (2015) 839–861.
[10] N. Rabbani, M. Xue, P.J. Thornalley, Methylglyoxal-induced dicarbonyl stress in aging and disease: first steps towards glyoxalase 1-based treatments, Clin. Sci. (Lond.) 130 (19) (2016) 1677–1696.
[11] J.A. Lin, C.H. Wu, C.C. Lu, S.M. Hsia, G.C. Yen, Glycative stress from advanced glycation end products (AGEs) and dicarbonyls: an emerging biological factor in cancer onset and progression, Mol. Nutr. Food Res. 60 (8) (2016) 1850–1864.
[12] C. Nigro, A. Leone, F. Fiory, I. Prevenzano, A. Nicolò, P. Mirra, et al., Dicarbonyl stress at the crossroads of healthy and unhealthy aging, Cells 8 (7) (2019) 749.
[13] R. Kold-Christensen, M. Johannsen, Methylglyoxal metabolism and aging-related disease: moving from correlation toward causation, Trends Endocrinol. Metab. 31 (2) (2020) 81–92.
[14] C. Prasad, K.E. Davis, V. Imrhan, S. Juma, P. Vijayagopal, Advanced glycation end products and risks for chronic diseases: intervening through lifestyle modification, Am. J. Lifestyle Med. 13 (4) (2019) 384–404.
[15] D. Schroter, A. Hohn, Role of advanced glycation end products in carcinogenesis and their therapeutic implications, Curr. Pharm. Des. 24 (44) (2018) 5245–5251.
[16] K. Yue, F.C.Y. Lee, Methylglyoxal may contribute to bone loss via differential effects on osteoblast and osteoclasts, Diabetes 68 (2019) ((Yue K.; Lee F.C.Y.) Hong Kong, Hong Kong).
[17] D. Vashishth, L. Karim, Effects of non-enzymatic glycation on trabecular bone fragility may be mediated through changes in bone matrix quality and microarchitecture, J. Bone Miner. Res. 25 (2010) ((Vashishth D.; Karim L.) Rensselaer Polytechnic Institute, United States):S72-S3.
[18] T. Aikawa, H. Matsubara, S. Ugaji, J. Shirakawa, R. Nagai, S. Munesue, et al., Contribution of methylglyoxal to delayed healing of bone injury in diabetes, Mol. Med. Rep. 16 (1) (2017) 403–409.
[19] S. Arakawa, R. Suzuki, D. Kurosaka, R. Ikeda, H. Hayashi, T. Kayama, et al., Mass spectrometric quantitation of AGEs and enzymatic crosslinks in human cancellous bone, Sci. Rep. 10 (1) (2020) 1–12.
[20] D. Yao, M. Brownlee, Hyperglycemia-induced reactive oxygen species increase expression of the receptor for advanced glycation end products (RAGE) and RAGE ligands, Diabetes 59 (1) (2010) 249–255.
[21] S.Y. Tang, D. Vashishth, Non-enzymatic glycation alters microdamage formation in human cancellous bone, Bone 46 (1) (2010) 148–154.
[22] S. Kume, S. Kato, S. Yamagishi, Y. Inagaki, S. Ueda, N. Arima, et al., Advanced glycation end-products attenuate human mesenchymal stem cells and prevent cognate differentiation into adipose tissue, cartilage, and bone, J. Bone Miner. Res. 20 (9) (2005) 1647–1658.
[23] K. Waqas, J. Chen, F. Koromani, K. Trajanoska, B.C.J. van der Eerden, A. G. Uitterlinden, et al., Skin autofluorescence, a noninvasive biomarker for advanced glycation end-products, is associated with prevalent vertebral and major osteoporotic fractures: the Rotterdam study, J. Bone Miner. Res. 35 (10) (2020) 1904–1913.
[24] S. Brings, T. Fleming, M. Freichel, M.U. Muckenthaler, S. Herzig, P.P. Nawroth, Dicarbonyls and advanced glycation end-products in the development of diabetic complications and targets for intervention, Int. J. Mol. Sci. 18 (5) (2017).
[25] L.I. Plotkin, A.L. Essex, H.M. Davis, RAGE signaling in skeletal biology, Curr. Osteoporos. Rep. 17 (1) (2019) 16–25.
[26] C. Bruedigam, M. Driel, M. Koedam, J. Peppel, B.C. van der Eerden, M. Eijken, Basic techniques in human mesenchymal stem cell cultures: differentiation into osteogenic and adipogenic lineages, genetic perturbations, and phenotypic analyses, Curr. Protoc. Stem Cell Biol. 17 (1) (2011), 1H-3.
[27] O. Abar, S. Dharmar, S.Y. Tang, The effect of aminoguanidine (AG) and pyridoxamine (pM) on ageing human cortical bone, Bone Joint Res. 7 (1) (2018) 105–110.
[28] O. Abar, S. Dharmar, S.Y. Tang, Aminoguanidine and pyridoxamine inhibit glucose-mediated ages formation in human cortical bone in vitro, J. Orthop. Res. 34 (2016) ((Abar O.; Dharmar S.; Tang S.Y.) Washington University in St. Louis, St. Louis, MO, United States).
[29] S.M. Sliman, T.D. Eubank, S.R. Kotha, M.L. Kuppusamy, S.I. Sherwani, E.S. Butler, et al., Hyperglycemic oxoaldehyde, glyoxal, causes barrier dysfunction, cytoskeletal alterations, and inhibition of angiogenesis in vascular endothelial cells: aminoguanidine protection, Mol. Cell. Biochem. 333 (1–2) (2010) 9–26.
[30] A.M. Brum, J. van de Peppel, C.S. van der Leije, M. Schreuders-Koedam, M. Eijken, B.C. van der Eerden, et al., Connectivity map-based discovery of parbendazole reveals targetable human osteogenic pathway, Proc. Natl. Acad. Sci. U. S. A. 112 (41) (2015) 12711–12716.
[31] W.H. Chan, H.J. Wu, N.H. Shiao, Apoptotic signaling in methylglyoxal-treated human osteoblasts involves oxidative stress, c-Jun N-terminal kinase, caspase-3, and p21-activated kinase 2, J. Cell. Biochem. 100 (4) (2007) 1056–1069.
[32] S. Delle Monache, F. Pulcini, R. Frosini, V. Mattei, V.N. Talesa, C. Antognelli, Methylglyoxal-dependent glycative stress is prevented by the natural antioxidant oleuropein in human dental pulp stem cells through Nrf2/Glo1 pathway, Antioxidants (Basel) 10 (5) (2021).
[33] R. Bielby, E. Jones, D. McGonagle, The role of mesenchymal stem cells in maintenance and repair of bone, Injury 38 (Suppl. 1) (2007) S26–S32.
[34] M.N. Knight, K.D. Hankenson, Mesenchymal stem cells in bone regeneration, Adv. Wound Care 2 (6) (2013) 306–316.
[35] M. Saito, Y. Kida, S. Kato, K. Marumo, Diabetes, collagen, and bone quality, Curr. Osteoporos. Rep. 12 (2) (2014) 181–188.
[36] M. Yamamoto, T. Sugimoto, Advanced glycation end products, diabetes, and bone strength, Curr. Osteoporos. Rep. 14 (6) (2016) 320–326.
[37] S. Franke, M. Sommer, C. Rüster, T. Bondeva, J. Marticke, G. Hofmann, et al., Advanced glycation end products induce cell cycle arrest and proinflammatory changes in osteoarthritic fibroblast-like synovial cells, Arthritis Res. Ther. 11 (5) (2009).
[38] Y.-J. Chen, D.-C. Chan, C.-K. Chiang, C.-C. Wang, T.-H. Yang, K.-C. Lan, Advanced Glycation End-products Induced VEGF Production and Inflammatory Responses in Human Synoviocytes via RAGE-NF-kappaB Pathway Activation, 2016.
[39] P.J. Thornalley, Use of aminoguanidine (Pimagedine) to prevent the formation of advanced glycation endproducts, Arch. Biochem. Biophys. 419 (1) (2003) 31–40.
[40] A.C. McLellan, P.J. Thornalley, J. Benn, P.H. Sonksen, Glyoxalase system in clinical diabetes mellitus and correlation with diabetic complications, Clin. Sci. (Lond.) 87 (1) (1994) 21–29.
[41] J. Scheijen, E. Clevers, L. Engelen, P.C. Dagnelie, F. Brouns, C.D.A. Stehouwer, et al., Analysis of advanced glycation endproducts in selected food items by ultra-performance liquid chromatography tandem mass spectrometry: presentation of a dietary AGE database, Food Chem. 190 (2016) 1145–1150.
[42] A. Lapolla, R. Reitano, R. Seraglia, G. Sartore, E. Ragazzi, P. Traldi, Evaluation of advanced glycation end products and carbonyl compounds in patients with different conditions of oxidative stress, Mol. Nutr. Food Res. 49 (7) (2005) 685–690.
[43] F.W. Chaplen, W.E. Fahl, D.C. Cameron, Evidence of high levels of methylglyoxal in cultured chinese hamster ovary cells, Proc. Natl. Acad. Sci. U. S. A. 95 (10) (1998) 5533–5538.
[44] K.S. Suh, E.M. Choi, S.Y. Rhee, Y.S. Kim, Methylglyoxal induces oxidative stress and mitochondrial dysfunction in osteoblastic MC3T3-E1 cells, Free Radic. Res. 48 (2) (2014) 206–217.
[45] Y. Qin, J. Guan, C. Zhang, Mesenchymal stem cells: mechanisms and role in bone regeneration, Postgrad. Med. J. 90 (1069) (2014) 643–647.
[46] J. Ribot, C. Denoeud, G. Frescaline, R. Landon, H. Petite, G. Pavon-Djavid, et al., Experimental type 2 diabetes differently impacts on the select functions of bone marrow-derived multipotent stromal cells, Cells 10 (2) (2021).
[47] F.C. Cassidy, C. Shortiss, C.G. Murphy, S.R. Kearns, W. Curtin, C. De Buitléir, et al., Impact of type 2 diabetes mellitus on human bone marrow stromal cell number and phenotypic characteristics, Int. J. Mol. Sci. 21 (7) (2020).
[48] H. Liu, X. Xia, B. Li, Mesenchymal stem cell aging: mechanisms and influences on skeletal and non-skeletal tissues, Exp. Biol. Med. (Maywood) 240 (8) (2015) 1099–1106.
[49] E. Aikawa, R. Fujita, M. Asai, Y. Kaneda, K. Tamai, Receptor for advanced glycation end products-mediated signaling impairs the maintenance of bone marrow mesenchymal stromal cells in diabetic model mice, Stem Cells Dev. 25 (22) (2016) 1721–1732.
[50] C. Antognelli, L. Marinucci, R. Frosini, L. Macchioni, V.N. Talesa, Metastatic prostate cancer cells secrete methylglyoxal-derived MG-H1 to reprogram human osteoblasts into a dedifferentiated, malignant-like phenotype: a possible novel player in prostate cancer bone metastases, Int. J. Mol. Sci. 22 (19) (2021).
[51] D.R. Eyre, M.A. Weis, Bone collagen: new clues to its mineralization mechanism from recessive osteogenesis imperfecta, Calcif. Tissue Int. 93 (4) (2013) 338–347.
[52] C.J. Harvey, R.K. Thimmulappa, A. Singh, D.J. Blake, G. Ling, N. Wakabayashi, et al., Nrf2-regulated glutathione recycling independent of biosynthesis is critical for cell survival during oxidative stress, Free Radic. Biol. Med. 46 (4) (2009) 443–453.
[53] H.K. Bryan, A. Olayanju, C.E. Goldring, B.K. Park, The Nrf2 cell defence pathway: Keap1-dependent and -independent mechanisms of regulation, Biochem. Pharmacol. 85 (6) (2013) 705–717.
[54] S.Y. Ko, S.S. Chang, I.H. Lin, H.I. Chen, Suppression of antioxidant Nrf-2 and downstream pathway in H9c2 cells by advanced glycation end products (AGEs) via ERK phosphorylation, Biochimie 118 (2015) 8–14.
[55] I.O. Sherif, The effect of natural antioxidants in cyclophosphamide-induced hepatotoxicity: role of Nrf2/HO-1 pathway, Int. Immunopharmacol. 61 (2018) 29–36.
[56] J. Xue, R. Ray, D. Singer, D. Bohme, D.S. Burz, V. Rai, et al., The receptor for advanced glycation end products (RAGE) specifically recognizes methylglyoxal-derived AGEs, Biochemistry 53 (20) (2014) 3327–3335.
[57] K.S. Suh, S. Chon, W.W. Jung, E.M. Choi, Crocin attenuates methylglyoxal-induced osteoclast dysfunction by regulating glyoxalase, oxidative stress, and mitochondrial function, Food Chem. Toxicol. 124 (2019) 367–373.
[58] T. Suantawee, T. Thilavech, H. Cheng, S. Adisakwattana, Cyanidin attenuates methylglyoxal-induced oxidative stress and apoptosis in INS-1 pancreatic β-cells by increasing Glyoxalase-1 activity, Nutrients 12 (5) (2020).
[59] F. Cipollone, A. Iezzi, M. Fazia, M. Zucchelli, B. Pini, C. Cuccurullo, et al., The receptor RAGE as a progression factor amplifying arachidonate-dependent inflammatory and proteolytic response in human atherosclerotic plaques: role of glycemic control, Circulation 108 (9) (2003) 1070–1077.
[60] A.M. Schmidt, O. Hori, J. Brett, S.D. Yan, J.L. Wautier, D. Stern, Cellular receptors for advanced glycation end products. Implications for induction of oxidant stress and cellular dysfunction in the pathogenesis of vascular lesions, Arterioscler. Thromb. 14 (10) (1994) 1521–1528.
[61] J.V. Valencia, M. Mone, C. Koehne, J. Reddiske, T.E. Hughes, Binding of receptor for advanced glycation end products (RAGE) ligands is not sufficient to induce inflammatory signals: lack of activity of endotoxin-free albumin-derived advanced glycation end products, Diabetologia 47 (5) (2004) 844–852.
[62] G. Sorci, F. Riuzzi, I. Giambanco, R. Donato, RAGE in tissue homeostasis, repair and regeneration, Biochim. Biophys. Acta 1833 (1) (2013) 101–109.
[63] R. Zhai, R. Blondonnet, E. Ebrahimi, C. Belville, J. Audard, C. Gross, et al., The receptor for advanced glycation end-products enhances lung epithelial wound repair: an in vitro study, Exp. Cell Res. 391 (2) (2020), 112030.

[64] C. Gross, C. Belville, M. Lavergne, H. Choltus, M. Jabaudon, R. Blondonnet, et al., Advanced glycation end products and receptor (RAGE) promote wound healing of human corneal epithelial cells, Invest. Ophthalmol. Vis. Sci. 61 (3) (2020) 14.
[65] N. Mizushima, M. Komatsu, Autophagy: renovation of cells and tissues, Cell 147 (4) (2011) 728–741.
[66] A. Takahashi, Y. Takabatake, T. Kimura, I. Maejima, T. Namba, T. Yamamoto, et al., Autophagy inhibits the accumulation of advanced glycation end products by promoting lysosomal biogenesis and function in the kidney proximal tubules, Diabetes 66 (5) (2017) 1359–1372.
[67] P. Hu, H. Zhou, M. Lu, L. Dou, G. Bo, J. Wu, et al., Autophagy plays a protective role in advanced glycation end product-induced apoptosis in cardiomyocytes, Cell. Physiol. Biochem. 37 (2) (2015) 697–706.
[68] R. Suzuki, Y. Fujiwara, M. Saito, S. Arakawa, J.I. Shirakawa, M. Yamanaka, et al., Intracellular accumulation of advanced glycation end products induces osteoblast apoptosis via endoplasmic reticulum stress, J. Bone Miner. Res. 35 (10) (2020) 1992–2003.
[69] D. Prantner, S. Nallar, K. Richard, D. Spiegel, K.D. Collins, S.N. Vogel, Classically activated mouse macrophages produce methylglyoxal that induces a TLR4- and RAGE-independent proinflammatory response, J. Leukoc. Biol. 109 (3) (2021) 605–619.
[70] S. Son, I. Hwang, S.H. Han, J.S. Shin, O.S. Shin, J.W. Yu, Advanced glycation end products impair NLRP3 inflammasome-mediated innate immune responses in macrophages, J. Biol. Chem. 292 (50) (2017) 20437–20448.
[71] Q. Li, B. Yu, P. Yang, Hypoxia-induced HMGB1 in would tissues promotes the osteoblast cell proliferation via activating ERK/JNK signaling, Int. J. Clin. Exp. Med. 8 (9) (2015) 15087–15097.
[72] N. Taniguchi, K. Yoshida, T. Ito, M. Tsuda, Y. Mishima, T. Furumatsu, et al., Stage-specific secretion of HMGB1 in cartilage regulates endochondral ossification, Mol. Cell. Biol. 27 (16) (2007) 5650–5663.